Adaptations of energy metabolism in cetaceans have consequences for their response to foraging disruption

Davina Derous[1*], Jagajjit Sahu[1], Alex Douglas[1] and David Lusseau[1], Marius Wenzel[2*]

1. Institute of Biological and Environmental Sciences, University of Aberdeen, Aberdeen, Scotland, UK
2. Centre for Genome Enabled Biology and Medicine, University of Aberdeen, Aberdeen, Scotland, UK

*Corresponding author:

DD: Email: davina.derous@abdn.ac.uk

Tel: +44 (0)1224 273637

DL: Email: d.lusseau@abdn.ac.uk

Tel: +44 (0)1224 272843

MW: Email: marius.wenzel@abdn.ac.uk

Tel: +44(0)1224 273471

Key words: cetaceans, mTOR, insulin, NF-κB, evolution, PCoD, PCoMS

Abstract

Cetaceans have varied their anatomical structure, physiology and metabolism to adapt to the challenges of aquatic life. Key to this change is the deposition of blubber. This adipose tissue plays a significant regulatory and signaling role in mammalian metabolism. As foraging disruption by human activities is emerging as a key conservation threat for cetaceans, we need to understand how selection for aquatic life might have altered key nutrient sensing pathways associated with adipose signaling. We compared selection pressure on those energy metabolism biological pathways by contrasting the rate of substitution observed in genes associated with them in cetacean and artiodactyl genomes. We then estimated the likely consequence of these selection pressures for pathway functions. Here we show that genes involved in the insulin, mTOR, SIRT and NF-κB pathways were under significant positive selection in cetaceans compared to their terrestrial sister taxon. Our results suggest these genes may have been positively selected to adapt to a glucose-poor diet and it is unlikely that fat depots signaling function in the same manner as in terrestrial mammals. Secondary adaptation to life in water significantly affected functions in nutrient sensing pathways in cetaceans. Insulin is not likely to play the same role in energy balance as it does in terrestrial mammals and adiposity is not likely to have the deleterious health consequences it has in terrestrial mammals. The physiological ecology of cetacean fat deposition, and therefore its value as a condition index, needs to be interpreted in this evolutionary context.

Introduction

Cetaceans are mammals that transitioned from a terrestrial to an aquatic lifestyle approximately 53–56 million years ago by adapting their anatomical structure, physiology and metabolism. These critical morphological and physiological adaptations ensured the maintenance of body temperature and energy reserves (Parry, 1949; Scholander, Walters, Hock, & Irving, 1950). For example, this included a thickening of the blubber (i.e. adipose tissue equivalent) to provide thermal insulation, to deal with more sporadic foraging opportunities, and to support locomotion (Vasseur & Yodzis, 2004; T M Williams, Friedl, & Haun, 1993; Terrie M. Williams, Haun, Davis, Fuiman, & Kohin, 2001). Crucially, these adaptations impact the ways in which individuals decide to invest in reproduction and define their abilities to survive under varied environmental pressures, in particular nutrient availability. Human-caused perturbations, such as shipping, tourism, naval activities, coastal urbanization and offshore energy development, can perturb environmental nutrient levels and affect cetacean foraging abilities. These factors are becoming a pervasive and prevalent threat to many cetacean species (Pirotta et al., 2018) and are a key priority in cetacean conservation policy (eg. National Academies of Sciences, Engineering, 2017).

Cetaceans detect fluctuations in environmental nutrient levels by nutrient sensing pathways and some of these are evolutionary conserved across species (Chantranupong, Wolfson, & Sabatini, 2015). These pathways detect intracellular and extracellular levels of sugar, amino acids and lipids and their surrogate metabolites. Nutrients can trigger the release of several hormones, which induce coherent responses in several pathways involved in regulating metabolism. Unsurprisingly, a large portion of positively selected genes in cetaceans are involved in energy metabolism (Nery, González, & Opazo, 2013). Bottlenose dolphins (*Tursiops truncatus*) show insulin resistance likely caused by early metabolic shifts in

64 substrate utilization as the species shifted from a terrestrial high carbohydrate diet to a
65 marine high protein diet (Wang et al., 2016). Dolphin diet has a high fat and protein content
66 and is almost devoid of carbohydrates (Wells et al., 2013). Fasted healthy bottlenose dolphins
67 (*Tursiops truncatus*) have elevated fasting plasma glucose concentration that are similar to
68 diabetic humans (S. Venn-Watson, Carlin, & Ridgway, 2011; S. K. Venn-Watson & Ridgway,
69 2007).. During fasting, metabolism is believed to be primarily fueled by large adipose stores
70 (i.e. blubber) that are mobilized in response to insulin suppression (Duncan, Ahmadian,
71 Jaworski, Sarkadi-Nagy, & Sul, 2007).

72 This fasting response is expected to take place when foraging is disrupted in the wild by
73 human activities. Regulatory genes related to lipolysis are positively selected in cetacean-
74 specific lineages but not in terrestrial mammals (Wang et al., 2015). Specifically, genes related
75 to triacylglycerol (TAG) metabolism were suggested to play an essential role in the secondary
76 adaption of cetaceans to aquatic life (Wang et al., 2015). The processes of lipid deposition
77 and utilization is regulated by the gene leptin (LEP) (Duncan et al., 2007). Recent work shows
78 that in bowhead whales (*Balaena mysticetus*) and belugas (*Delphinapterus leucas*), the
79 regulation of LEP and lipolysis is adapted to seasonal cycles of blubber deposition and
80 utilization (Ball et al., 2017). Although adipose tissue biology of terrestrial mammals show a
81 similarity to the functioning of cetacean blubber, some differences in key genes have been
82 identified (Ball et al., 2017). These changes have therefore the scope to alter the way
83 individual take biological decisions about demographic contributions, particularly
84 reproduction, given their energetic metabolic state. We need to place gene selection in the
85 context of the biological pathways in which they are involved to contextualize those changes
86 and understand the potential demographic consequences of foraging disruption when the
87 environmental nutrient levels of cetaceans are perturbed. Here, we aimed to determine

whether the selective pressure from secondary adaptations to life in water led to a change in the key nutrient signaling pathways. We aim to predict whether these changes are likely to affect biological functions.

Material and Methods

To understand the evolutionary-driven changes in the regulation of metabolic processes in cetaceans, we took a targeted approach and focused on 6 signaling pathways: the p53 signaling pathway, the insulin signaling pathway, the mTOR signaling pathway, the leptin signaling pathway, the NF-κB signaling pathway and the SIRT signaling pathway. A total of 532 genes involved in these pathways were obtained from the Kyoto Encyclopedia of Genes and Genomes (KEGG) website (http://www.genome.jp/kegg/) and from the Ingenuity Pathway Analysis (IPA) program (version 2000-2019, Ingenuity Systems, www.ingenuity.com).

Analysis of positive gene selection and amino-acid substitutions

We obtained the full amino-acid sequences from 532 human KEGG proteins included in our pathways of interest and downloaded from *NCBI* the genome assemblies of human, mouse, 16 cetacean species and 37 artiodactyl species (Table S1). We aligned the KEGG proteins to all genomes using *EXONERATE* 2.2.0 (Slater & Birney, 2005) with the *protein2genome* model to allow for spliced alignments across introns. For each genome, the single match with the highest alignment score was retained and the nucleotide sequence of the match was extracted. If multiple best matches with the same score were present, one match was chosen at random. Sequences were codon-aligned with guidance from corresponding amino-acid alignments and allowing for frame-shifts using *MACSE* 2.03 (Ranwez, Douzery, Cambon, Chantret, & Delsuc, 2018), and maximum-likelihood gene trees were inferred in *IQTREE* 1.6.8

(Nguyen, Schmidt, Von Haeseler, & Minh, 2015) with automatic selection of nucleotide substitution models. A species tree was then inferred from all 532 gene trees using *ASTRAL-III* 5.6.3 (Zhang, Rabiee, Sayyari, & Mirarab, 2018) and rooted at the two outgroups human and mouse.

Codon sequence evolution was modelled in the *codeml* program of *PAML* 4.9f (Yang, 2007), using the species tree with a trifurcated root (=derooted). To minimize the impact of missing data, all codons with more than 20 % missing data were removed from the alignments using *TRIMAL* 1.4 (Capella-Gutiérrez, Silla-Martínez, & Gabaldón, 2009). Three types of models were run per alignment. First, the null model estimated a single dN:dS ratio (ω) for the entire alignment. Second, the branch model (model = 2; NSsites = 0) estimated a single ω for all cetacean lineages (foreground) and a second ω for all other lineages (background). Third, the branch-site model (model = 2; NSsites = 2) estimated different ω among codons within the foreground and background branches. The branch models and branch-site models were each run twice, either allowing the foreground ω to vary freely or fixing ω at 1 (=neutral evolution). The statistical significance of the free ω estimates of interest was obtained via likelihood-ratio tests carried out in *R* 3.4.0 (R Core Team, 2014). Both the free branch model and the free branch-site model were contrasted with their corresponding neutral models and with the null model by comparing twice the difference in likelihood ($2\Delta L$) of the models against a *Chi*-square distribution with one degree of freedom. *P*-values were corrected for multiple testing across all genes within each type of contrast using the false-discovery-rate method (Benjamini & Hochberg, 1995).

From all branch-site models with free ω that fitted significantly better than the neutral branch-site model and the null model, we identified the specific codons under positive selection in the cetacean lineage using the Bayes Empirical Bayes (BEB) method (Yang, 2007).

We then examined whether the amino-acid substitutions in the cetacean lineage at these sites would have detrimental effects on the function of the protein using *PROVEAN* 1.1.5 (Choi, Sims, Murphy, Miller, & Chan, 2012). For each protein, the *Homo sapiens* sequence was used as the reference sequence, and the single most frequent alternative amino acid observed among the 16 cetacean genomes was queried.

Pathway level comparison

The value of statistically significant likelihood-ratio test statistics (2ΔL) between the positive and neutral branch-models were used as a measure to visualize the interactions of the positive gene selection at a pathway level using IPA signaling pathways for each of the target pathway (version 2000-2019, Ingenuity Systems, www.ingenuity.com). IPA did not have a prebuilt sirtuin signaling pathway. We therefore manually constructed this pathway based on the summarized data by Nakagawa and Guarente (2011) (Nakagawa & Guarente, 2011).

Prediction of functional effects

Deleterious amino acid substitutions (PROVEAN scores <= -2.5) in positively selected codons were visualized using IPA and possible downstream effects in the pathways based on the damaged protein were predicted using the Molecule Activity Predictor (MAP) function in IPA.

Results

Strength of selective pressure on genes involved in nutrient sensing pathways

The species tree inferred from all gene trees (Fig 1) was consistent with published cetacean and artiodactylan phylogenies (Zurano et al., 2019). Alignment-wide ω estimates from the PAML null models were <1 for all but one gene (median: 0.08; mean: 0.12), consistent with a baseline of strong purifying selection on protein function across all taxa and all codons (Fig 2A). Contrasting the cetacean group with all other taxa using branch models revealed that 224 out of 532 genes (42.1 %) departed significantly ($q \leq 0.05$) from neutral codon evolution ($\omega \neq 1$), but all of these genes were under purifying selection ($\omega < 1$) instead of positive selection ($\omega > 1$). Only seven genes were candidates for positive selection ($\omega > 1$), but none of these estimates were significant (Fig 2B). In contrast, branch-site models revealed significant ($q \leq 0.05$) positive selection ($\omega > 1$; median: 9.67; mean: 39.64) in the cetacean group on a small subset of codons in 133 of 532 genes (25 %) (Fig 2C).

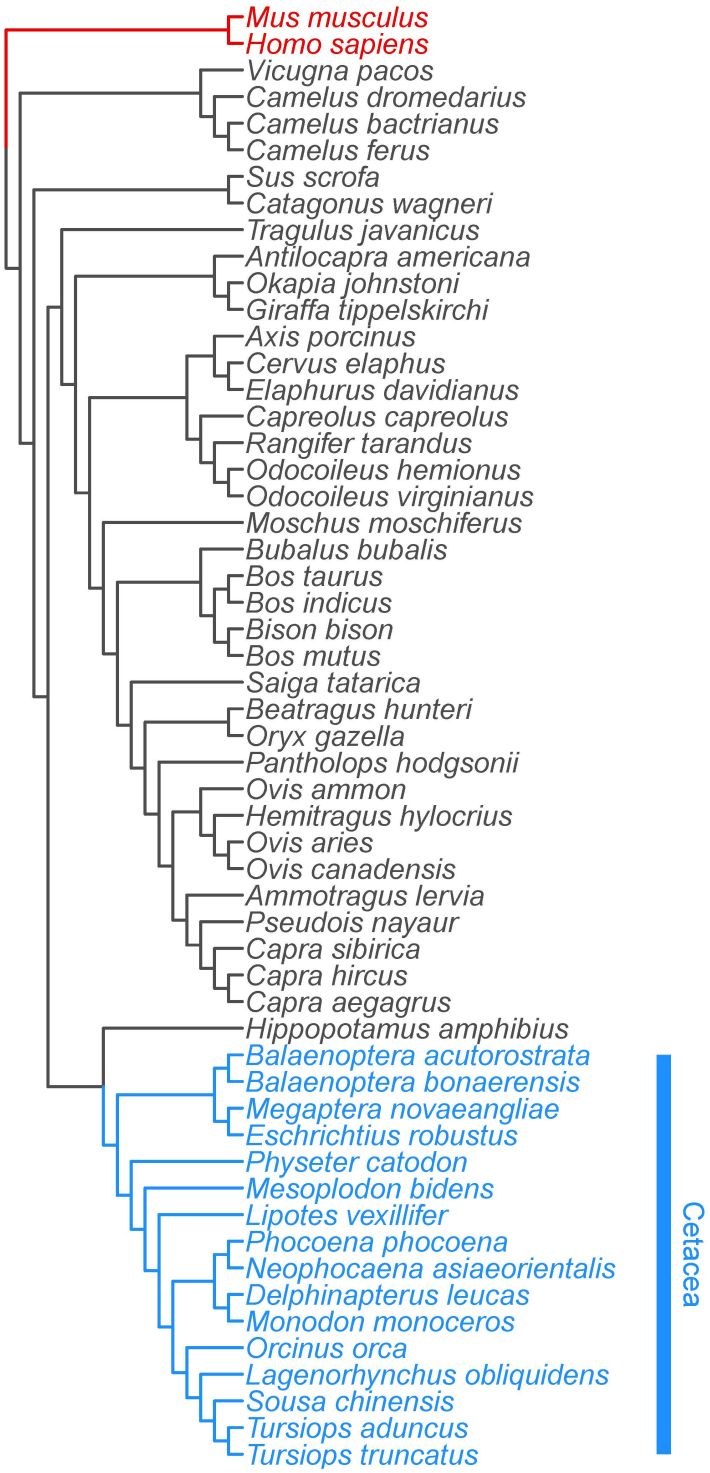

Figure 1. Species cladogram of the cetacea ingroup (blue) and artiodactyla, human and mouse outgroups (black and red), derived from 532 gene alignments.

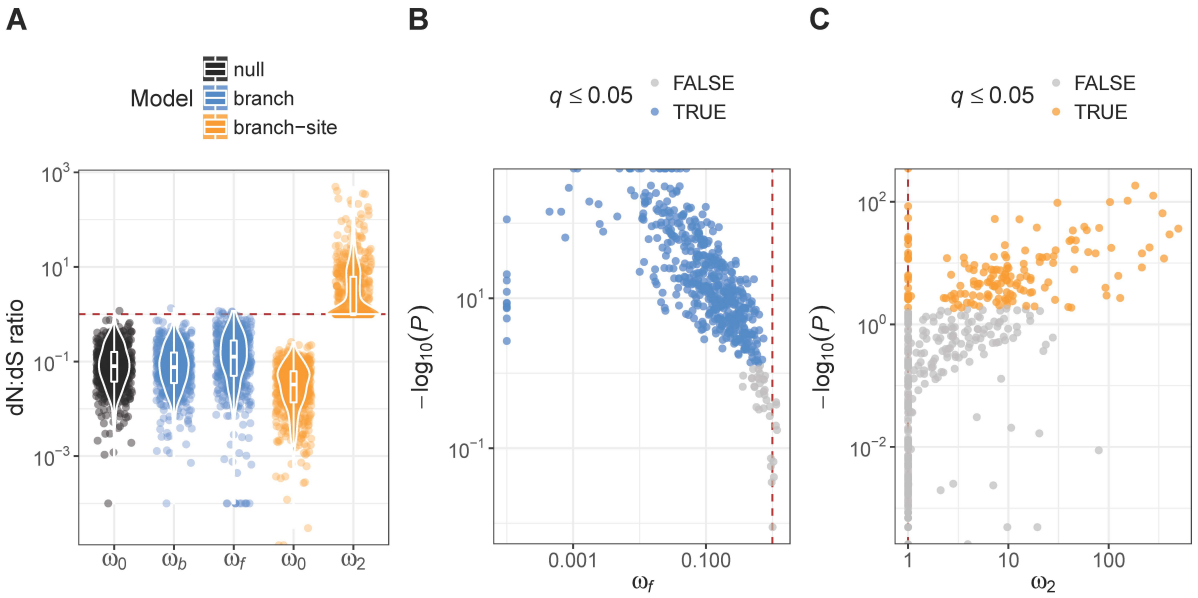

Figure 2: Ratios of non-synonymous vs. synonymous nucleotide substitution rates (dN:dS ratios; ω) in 532 genes estimated from codon evolution models in PAML. A) baseline estimates for whole alignments from null models (ω0), estimates for foreground (cetacea; ωf) and background (all others; ωb) branches from branch models, and estimates for codons under purifying (ω0) and positive (ω2) selection in foreground branch (cetacea) from branch-site models. B) Foreground dN:dS ratio (ωf) and statistical significance (*P*-value) from likelihood-ratio tests between free-ratio branch models and neutral branch models. Significant tests after FDR correction (q ≤ 0.05) are highlighted in blue. C) Foreground dN:dS ratio of positively selected codons (ω2) and statistical significance (P-value) from likelihood-ratio tests between positive-selection branch-site models and neutral branch-site models. Significant tests after FDR correction (q ≤ 0.05) are highlighted in orange. The red dashed lines in all plots represent neutral evolution (ω =1).

Positive gene selection at the pathway level

We then visualized the interactions of the positive gene selection at a pathway level using IPA signaling pathways. Insulin signaling (Fig S1, Table S2), mTOR signaling (Fig S2, Table S3), NF-κB signaling (Fig S3, Table S4) and SIRT signaling (Fig S4, Table S5) were found to be positively selected, especially those related to glucose metabolism and inflammation. Genes particularly upstream from lipid metabolism, cell growth and proliferation and apoptosis functions were positively selected in the cetacean lineage. Little differences in selection were found for p53 signaling (Fig S5, Table S6) and leptin signaling (Fig S6, Table S7).

195 *Prediction of functional effects*

196 Using the BEB method in PAML, a total of 1936 codons among the 133 genes positively
197 selected in the cetacean lineage (mean 14.78 codons per gene) were under positive selection.
198 The predicted functional effects of the amino-acid substitutions in cetacea were
199 predominantly deleterious (median provean score: -2.9) and only 8.5 % of substitutions had
200 a positive score (Fig 3).

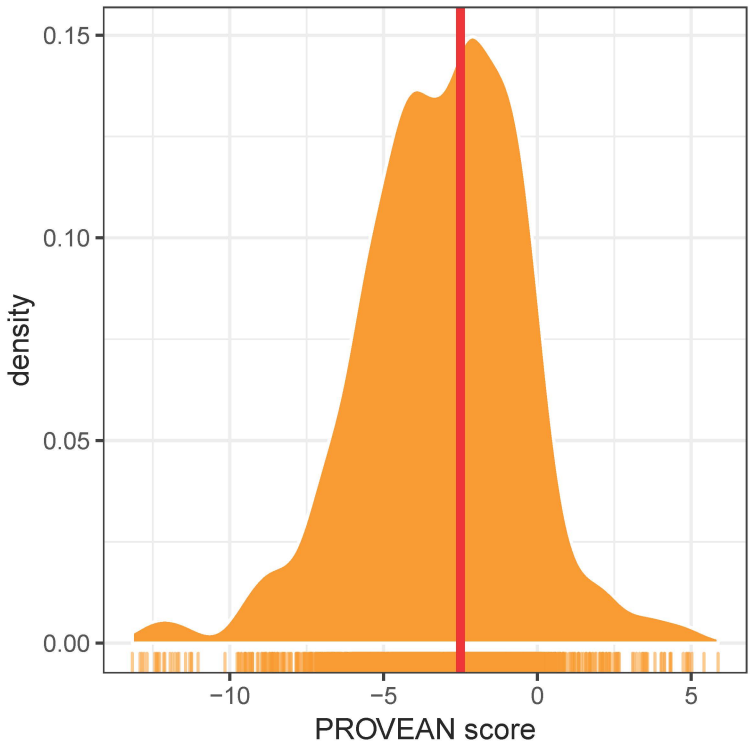

201
202 Figure 3. Distribution of *PROVEAN* scores of 1936 amino-acid substitutions under positive
203 selection in cetacea. The red line indicates the standard threshold (-2.5) below which the
204 effect of a substitution is considered deleterious.
205
206 These deleterious effects were likely to impact the way biological processes function.
207 Unsurprisingly, glucose metabolism is expected to be altered with changes in insulin signaling
208 (Fig 4), SIRT3 signaling with downstream regulation of insulin sensitivity, PPARA signaling with
209 downstream regulation of gluconeogenesis and oxidation of fatty acids (Fig 5). In addition, we
210 expect changes in upstream signaling of inflammation, hypoxia and cell survival via SIRT6,
211 RB1, NFKB and HIF1a (Fig 5&6). Importantly, both the mTOR complexes and its upstream and
212 downstream genes were estimated to be changed (Fig 7). The changes would have effects on
213 nutrient sensing and protein synthesis as well as key biological decisions about energetic
214 investment such as shift to glycolysis and de novo lipid synthesis.

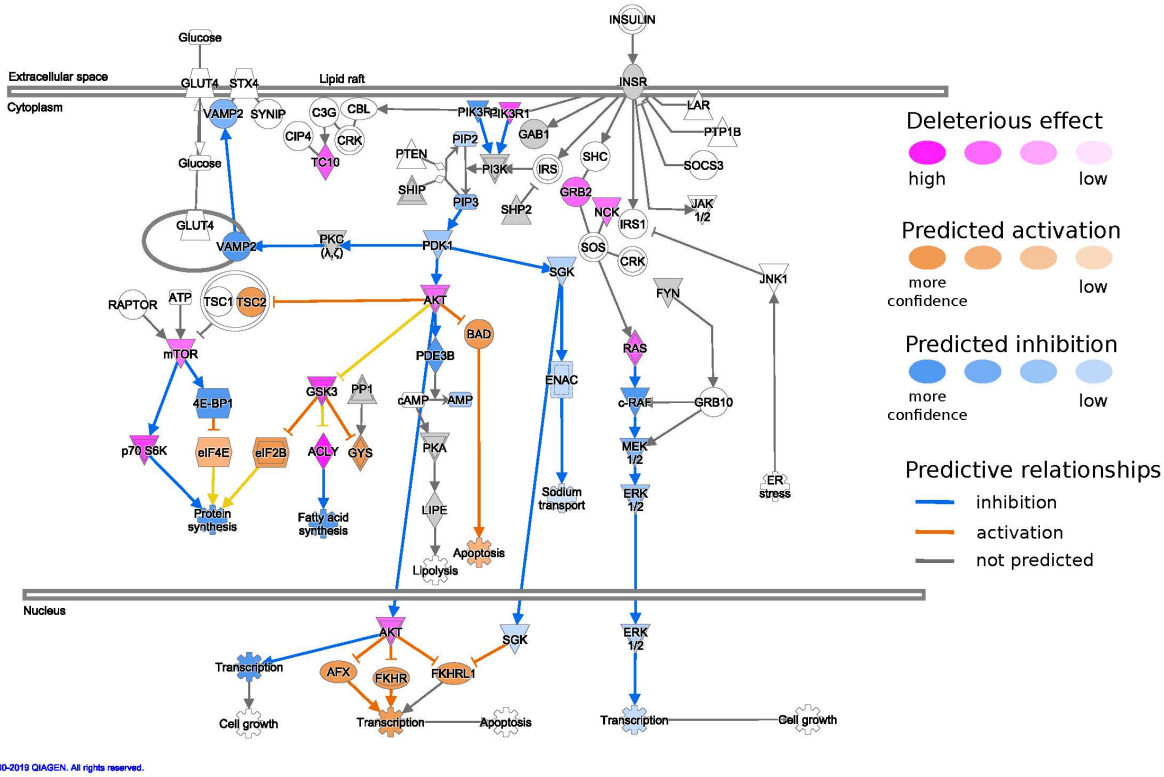

Figure 4. The insulin signaling pathway obtained from the Ingenuity Pathway Analysis (IPA) program. Genes with a damaging amino acid substitution are colored in magenta. Possible downstream damaging effects of these genes were visualized using the Molecule Activity Predictor (MAP) tool in IPA (see prediction legend).

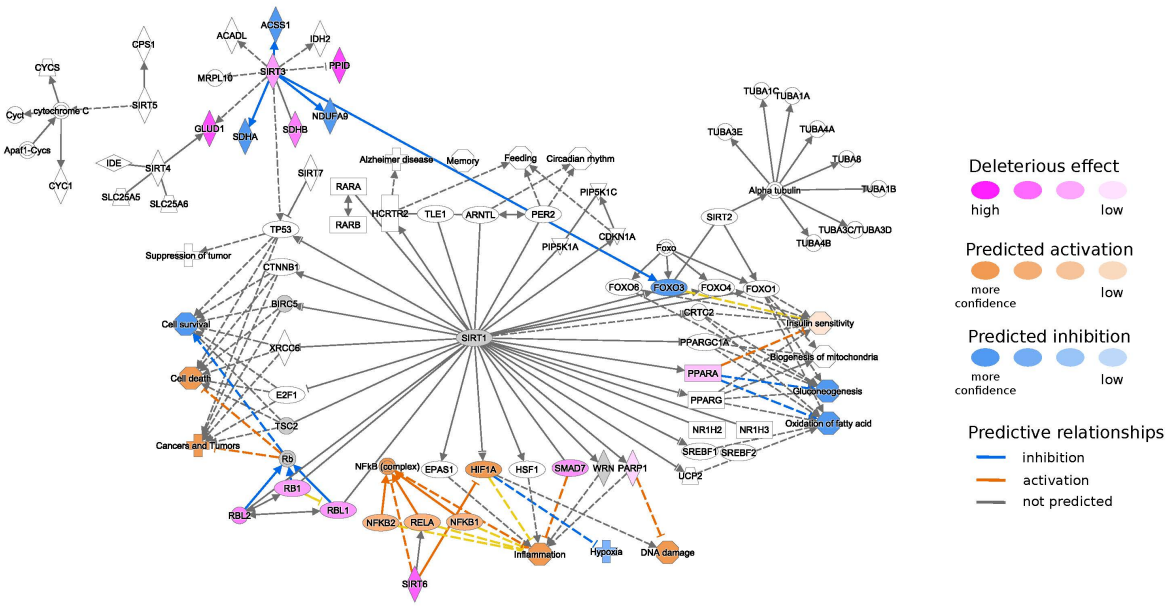

Figure 5. The SIRT signaling pathway obtained from the Ingenuity Pathway Analysis (IPA) program. Genes with a damaging amino acid substitution are colored in magenta. Possible

225 downstream damaging effects of these genes were visualized using the Molecule Activity
226 Predictor (MAP) tool in IPA (see prediction legend).

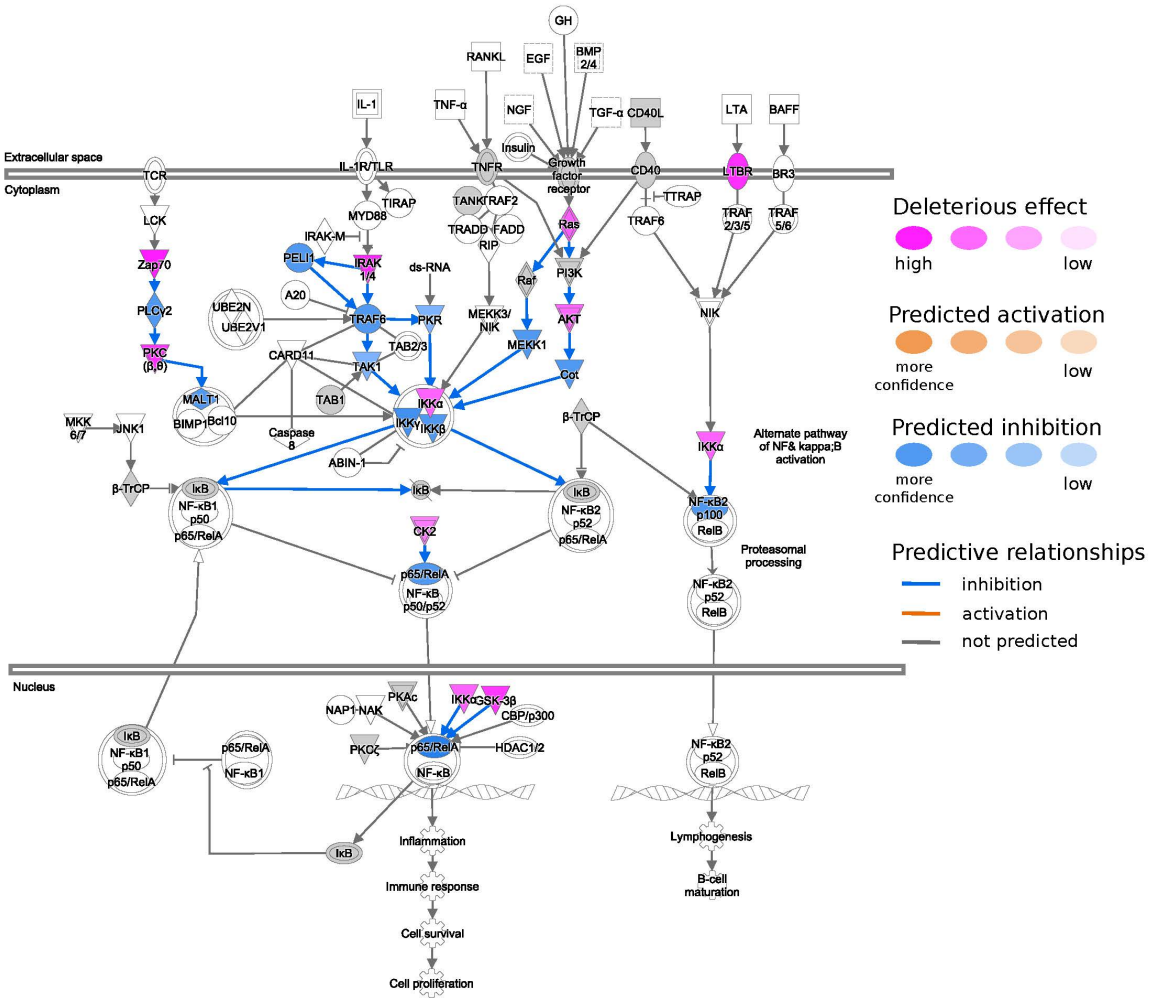

227
228 Figure 6. The NF-κB signaling pathway obtained for Ingenuity Pathway Analysis (IPA) program.
229 Genes with a damaging amino acid substitution are colored in magenta. Possible downstream
230 damaging effects of these genes were visualized using the Molecule Activity Predictor (MAP)
231 tool in IPA (see prediction legend).

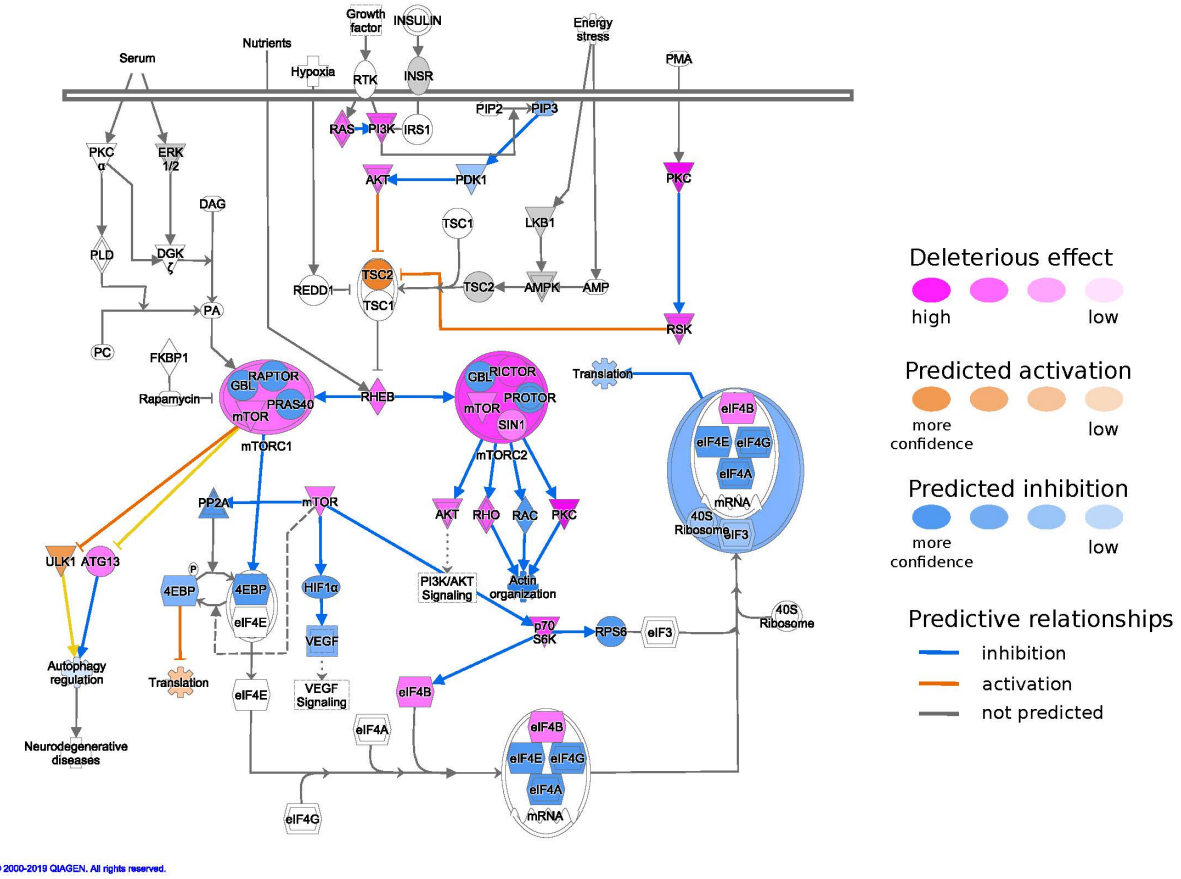

Figure 7. The mTOR signaling pathway obtained for Ingenuity Pathway Analysis (IPA) program. Genes with a damaging amino acid substitution are colored in magenta. Possible downstream damaging effects of these genes were visualized using the Molecule Activity Predictor (MAP) tool in IPA (see prediction legend).

Discussion

Here we took a targeted approach to identify positive selected genes in cetacean nutrient sensing pathways. This allowed us to better understand how combined changes might be focused on particular functions within these pathways and what the consequences of these changes might be for the way by which energy metabolism in cetaceans may differ from their terrestrial counterparts. These pathways have signaling cascades in common with hormones such as insulin and are linked with the release of hormones from adipose tissue (e.g. leptin). Our results indicate that genes involved in the insulin signaling pathway, the mTOR, SIRT and NF-κB signaling pathway were significantly positively selected. These

247 pathways have profound effects on metabolism and the maintenance of energy reserves. In
248 terrestrial mammals, adipose tissue mass is related to metabolic fitness and expansion can
249 lead to inflammation triggering metabolic disfunctions and diseases (e.g. obesity, metabolic
250 syndrome, insulin resistance). The positive selection of genes related to glucose metabolism
251 and inflammation suggest that these genes may have been positively selected to adapt to a
252 glucose-poor diet and that fat deposits signaling may not be as limited by inflammation,
253 metabolic dysfunctions (e.g. insulin resistance) and reproduction. Understanding these
254 adaptations can help us manage conservation threats that perturb the environmental
255 nutrient levels of cetaceans (National Academies of Sciences, Engineering, 2017).

256 Cetaceans have a diet with a high fat and protein content and is almost devoid of
257 carbohydrates (Wells et al., 2013). Hence pathways regulating carbohydrate and glucose
258 metabolism would have been under selective pressure as these species underwent a shift in
259 substrate utilization. Genes related to the control of food intake, glycerol uptake and glucose
260 metabolism were found to be under positive selective pressure in dolphins (McGowen,
261 Grossman, & Wildman, 2012). A high glucose transport may be needed via erythrocytes to
262 deliver glucose to specific brain regions under normal or physiological stress conditions (e.g.
263 hypoxia while diving) (Craik, Young, & Cheeseman, 1998). We found positive selections in the
264 insulin signaling pathway which are consistent with this hypothesis. In fasted Northern
265 elephant seals components of the insulin signaling pathway were reduced including glucose
266 transport (GLUT4), phosphatidylinositol 3-kinase (PI3K) and phosphorylated insulin receptor
267 substrate 1 (IRS1) (Viscarra, Vázquez-Medina, Crocker, & Ortiz, 2011). In our study, both PI3K
268 and IRS1 genes were estimated to be under positive selection but not GLUT4.-Elephant seals
269 are also insulin resistant (Viscarra et al., 2011) and hence may share common evolutionary
270 selection of those mechanisms with cetaceans. We indeed identified deleterious changes to

the insulin signaling pathway, including the Akt protein signaling kinase (Akt) and PI3K. Damage to this pathway in various tissues has been linked to insulin resistance (Huang, Liu, Guo, & Su, 2018). The three Akt isoforms have differential physiological functions but loss of function in one isoform is compensated by another. Both $Akt2^{-/-}$ and $Akt3^{-/-}$ mice exhibit severe glucose and insulin resistance (Dummler et al., 2006). Interestingly the Akt phosphorylation at Ser473, which is required for its full activation, is accomplished by mTORC2 (Oh & Jacinto, 2011; Sarbassov, Guertin, Ali, & Sabatini, 2005). Both mTORC1 and mTORC2 were positively selected in the cetacean lineage to a point where we cannot expect them to function in the same way as in terrestrial mammals. In addition to PI3K/AKT signaling, PPARα was also positively selected. Activation of the PPARα isoform leads to improved lipid and carbohydrate profile and to reduced inflammation (Moller & Berger, 2003). It's anti-inflammatory properties have been linked to the suppression of NF-κB (Fuentes, Guzmán-Jofre, Moore-Carrasco, & Palomo, 2013). However, PPARα is predominantly involved in cellular uptake, activation and β-oxidation of fatty acids (Moller & Berger, 2003). $PPAR\alpha^{-/-}$ mice exposed to long-term high fat diet remained normoglycemic and normoinsulinemic despite having high adiposity while the wild type developed hyperinsulemia. In addition, glucose and insulin tolerance test indicated that high-fat-fed wild type developed insulin resistance over time while the $PPAR\alpha^{-/-}$ remained unchanged (Guerre-Millo et al., 2001). Hence in absence of PPARα, the increase in adiposity as a result of a high fat diet does not lead to insulin resistance. Interestingly, when dolphins were fed a big meal of fish, they do show signs of insulin resistant (Venn-Watson et al., 2011). However, when just fed dextrose and water they showed an insulin-deficient response (S. Venn-Watson et al., 2013). This response to glucose is similar to the GTT test of the $PPAR\alpha^{-/-}$ mice. Hence key genes such as PPARα, AKT and PI3K in the insulin signaling pathway may be positively selected as an

295 evolutionary driver for insulin resistance and to switch between type 2 and type 1 diabetes
296 like states (S. Venn-Watson, 2014).

297 Maintaining adiposity can have negative consequences for survival in terrestrial
298 mammals. We know that a large volume of adipose tissue triggers inflammatory responses in
299 a range of species and can lead to metabolic dysfunctions at a physiological level (e.g. insulin
300 resistance) (Mantovani, Sozzani, Locati, Allavena, & Sica, 2002). NF-κB is involved in the
301 molecular signaling of hypoxia during adipose tissue expansion and triggers these
302 inflammatory responses (Ye, Gao, Yin, & He, 2007). As the inflammatory function of NF-κB is
303 linked to fat mass, the high level of adiposity in cetaceans would lead to chronic inflammation.
304 The thickened blubber of cetaceans is a result of the secondary adaptation to life in water and
305 hence selective pressure in this pathway may be a way to reduce intrinsic tissue inflammation.
306 Here we found that key genes in the NF-κB signaling pathway were positively selected
307 inhibitor of nuclear factor kappa B kinase subunit beta (IKKβ) and IKKα. Mice that have the
308 inflammatory pathway of NF-κB disabled (IKKβ knockout) are more insulin sensitive and are
309 partially protected from high fat diet induced glucose intolerance and hyperinsulinemia
310 (Arkan et al., 2005). In addition, the gene regulation of receptor interacting serine/threonine
311 kinase 1 (RIPK1) was also positively selected and its associated amino acid sequence changed
312 drastically compared to the outgroups. RIPK1 has a downstream effect on IKKα and IKKβ, and
313 hence may influence the signaling in this pathway. The IKK complex has a NF-κB independent
314 role in the protection of cells from RIPK–dependent death downstream from the tumor
315 necrosis factor rector (TNFR1) (Dondelinger et al., 2015). Cetaceans do have a fully
316 functioning immune and endocrine responses and these are highly dependent on the
317 environment (e.g. pathogens, pollution and noise) (Fair & Becker, 2000; Fair et al., 2017). For
318 example transcripts encoding pro-inflammatory cytokines were significantly lower in

319 managed-care dolphins compared to free-ranging dolphins (Fair et al., 2017). A greater
320 understanding of tissue specific inflammatory responses is needed and may provide valuable
321 insights into how inflammatory responses are regulated in regards to the high adiposity in
322 these healthy but “obese” mammals, during periods of diving and environmental fluctuation.

323 Finally, most components in the mTOR pathway were positively selected including
324 both of its complexes (mTORC1 and mTORC2). mTORC1 regulates processes related to growth
325 and differentiation while mTORC2 plays a regulatory role in the insulin cascade (Lamming et
326 al., 2012). mTOR is primarily involved in immune response and sensing nutrient availability.
327 As elevated mTOR leads to increased hepatic gluconeogenesis and reduced glucose uptake
328 by muscles, it is maybe not surprising that several components in the mTOR pathway are
329 significantly changed in cetaceans. Especially as mTOR is involved in nutrient sensing. As
330 dolphins are able to switch between type 2 and type 1 diabetes like states based on their meal
331 content (S. Venn-Watson, 2014), specific components both up- and down- stream from mTOR
332 may be positively selected to facilitate such a response. In rats, a ketogenic diet (low in
333 carbohydrates) are able to reduce mTOR expression and likely via AKT (McDaniel, Rensing,
334 Thio, Yamada, & Wong, 2011). Rodents fed on a keto diet also exhibit lower insulin levels,
335 which likely induce a decreased mTOR signaling (Thio, Erbayat-Altay, Rensing, & Yamada,
336 2006). Cetaceans have a diet similar to ketogenic diet with a high fat and protein content and
337 almost devoid of carbohydrates (Wells et al., 2013). Hence, to optimise the uptake of the
338 limited available glucose in the diet, aspects in the insulin/mTOR pathway may be altered to
339 create insulin resistance.

340

Conclusion

Taken together, our findings provide novel insights into the role of the insulin, mTOR and NF-κB signaling pathways in the adaptation of cetaceans to an aquatic life. They point to adaptations likely to reduce the health consequences of adiposity. These results mean that condition measures based on adiposity must be used with caution. Indeed, lower bounds of adiposity are influenced by thermoregulatory requirements and upper bounds of adiposity will not be influenced by inflammatory response in the same way as it is in terrestrial mammals.

Further work is needed to unravel the complex signaling mechanisms of adipose tissue in cetacean energy metabolism and to determine the effects of these signaling molecules on whole body functioning including appetite regulation, energy balance, and inflammatory responses. Understanding these adaptations can help us manage conservation threats that perturb the environmental nutrient levels of cetaceans (National Academies of Sciences, Engineering, 2017).

Authors' Contributions

DL, JS and DD designed the study. DD wrote the manuscript and performed the pathway level analyses and interpretation with input from DL. MW performed the gene-level analyses with input from AD and JS. DD, MW and DL interpreted the data. All authors read and commented on the manuscript.

Acknowledgements

This work was funded by US ONR grant award number N000141512377. The authors acknowledge the support of the Maxwell computer cluster funded by the University of Aberdeen.

Data accessibility

Data will become openly available after uploading on Dryad.

References

Arkan, M. C., Hevener, A. L., Greten, F. R., Maeda, S., Li, Z.-W., Long, J. M., … Karin, M. (2005). IKK-beta links inflammation to obesity-induced insulin resistance. *Nature Medicine*, *11*(2), 191–8. doi:10.1038/nm1185

Ball, H. C., Londraville, R. L., Prokop, J. W., George, J. C., Suydam, R. S., Vinyard, C., … Duff, R. J. (2017). Beyond thermoregulation: metabolic function of cetacean blubber in migrating bowhead and beluga whales. *Journal of Comparative Physiology B*, *187*(1), 235–252. doi:10.1007/s00360-016-1029-6

Benjamini, Y., & Hochberg, Y. (1995). Controlling the false discovery rate: a practical and powerful approach to multiple testing. *Journal of the Royal Statistical Society. Series B …*, *57*(1), 289–300. doi:10.2307/2346101

Capella-Gutiérrez, S., Silla-Martínez, J. M., & Gabaldón, T. (2009). trimAl: A tool for automated alignment trimming in large-scale phylogenetic analyses. *Bioinformatics*. doi:10.1093/bioinformatics/btp348

Chantranupong, L., Wolfson, R. L., & Sabatini, D. M. (2015). Nutrient-sensing mechanisms across evolution. *Cell*, *161*(1), 67–83. doi:10.1016/j.cell.2015.02.041

Choi, Y., Sims, G. E., Murphy, S., Miller, J. R., & Chan, A. P. (2012). Predicting the Functional Effect of Amino Acid Substitutions and Indels. *PLoS ONE*, *7*(10). doi:10.1371/journal.pone.0046688

Craik, J. D., Young, J. D., & Cheeseman, C. I. (1998). GLUT-1 mediation of rapid glucose

386 transport in dolphin (Tursiops truncatus) red blood cells. *The American Journal of*
387 *Physiology*, *274*(1 Pt 2), R112-9.

388 Dondelinger, Y., Jouan-Lanhouet, S., Divert, T., Theatre, E., Bertin, J., Gough, P. J., …
389 Bertrand, M. J. M. (2015). NF-κB-Independent Role of IKKα/IKKβ in Preventing RIPK1
390 Kinase-Dependent Apoptotic and Necroptotic Cell Death during TNF Signaling.
391 *Molecular Cell*, *60*(1), 63–76. doi:10.1016/j.molcel.2015.07.032

392 Dummler, B., Tschopp, O., Hynx, D., Yang, Z.-Z., Dirnhofer, S., & Hemmings, B. A. (2006). Life
393 with a single isoform of Akt: mice lacking Akt2 and Akt3 are viable but display impaired
394 glucose homeostasis and growth deficiencies. *Molecular and Cellular Biology*, *26*(21),
395 8042–51. doi:10.1128/MCB.00722-06

396 Duncan, R. E., Ahmadian, M., Jaworski, K., Sarkadi-Nagy, E., & Sul, H. S. (2007). Regulation of
397 lipolysis in adipocytes. *Annual Review of Nutrition*, *27*, 79–101.
398 doi:10.1146/annurev.nutr.27.061406.093734

399 Fair, P. A., & Becker, P. R. (2000). Review of stress in marine mammals. *Journal of Aquatic*
400 *Ecosystem Stress and Recovery*, *7*(4), 335–354. doi:10.1023/A:1009968113079

401 Fair, P. A., Schaefer, A. M., Houser, D. S., Bossart, G. D., Romano, T. A., Champagne, C. D., …
402 Reif, J. S. (2017). The environment as a driver of immune and endocrine responses in
403 dolphins (Tursiops truncatus). *PloS One*, *12*(5), e0176202.
404 doi:10.1371/journal.pone.0176202

405 Fuentes, E., Guzmán-Jofre, L., Moore-Carrasco, R., & Palomo, I. (2013, December 1). Role of
406 PPARs in inflammatory processes associated with metabolic syndrome (Review).
407 *Molecular Medicine Reports*. Spandidos Publications. doi:10.3892/mmr.2013.1714

Guerre-Millo, M., Rouault, C., Poulain, P., Andre, J., Poitout, V., Peters, J. M., … Staels, B. (2001). PPAR-/-Null Mice Are Protected From High-Fat Diet-Induced Insulin Resistance. *Diabetes*, *50*(12), 2809–2814. doi:10.2337/diabetes.50.12.2809

Huang, X., Liu, G., Guo, J., & Su, Z. (2018). The PI3K/AKT pathway in obesity and type 2 diabetes. *International Journal of Biological Sciences*, *14*(11), 1483–1496. doi:10.7150/ijbs.27173

Lamming, D. W., Ye, L., Katajisto, P., Goncalves, M. D., Saitoh, M., Stevens, D. M., … Sancak, Y. (2012). Rapamycin-induced insulin resistance is mediated by mTORC2 loss and uncoupled from longevity. *Science*, *335*, 1638–43. doi:10.1126/science.1215135

Mantovani, A., Sozzani, S., Locati, M., Allavena, P., & Sica, A. (2002). Macrophage polarization: tumor-associated macrophages as a paradigm for polarized M2 mononuclear phagocytes. *Trends in Immunology*, *23*(11), 549–555. doi:10.1016/S1471-4906(02)02302-5

McDaniel, S. S., Rensing, N. R., Thio, L. L., Yamada, K. A., & Wong, M. (2011). The ketogenic diet inhibits the mammalian target of rapamycin (mTOR) pathway. *Epilepsia*, *52*(3), e7-11. doi:10.1111/j.1528-1167.2011.02981.x

McGowen, M. R., Grossman, L. I., & Wildman, D. E. (2012). Dolphin genome provides evidence for adaptive evolution of nervous system genes and a molecular rate slowdown. *Proceedings of the Royal Society B: Biological Sciences*, *279*(1743), 3643–3651. doi:10.1098/rspb.2012.0869

Moller, D. E., & Berger, J. P. (2003). Role of PPARs in the regulation of obesity-related insulin sensitivity and inflammation. *International Journal of Obesity*, *27*(S3), S17–S21.

430 doi:10.1038/sj.ijo.0802494

431 Nakagawa, T., & Guarente, L. (2011). Sirtuins at a glance. *Journal of Cell Science*, *124*(6),
432 833–838. doi:10.1242/jcs.081067

433 National Academies of Sciences, Engineering, and M. (2017). *Approaches to Understanding*
434 *the Cumulative Effects of Stressors on Marine Mammals*. Washington, D.C.: National
435 Academies Press. doi:10.17226/23479

436 Nery, M. F., González, D. J., & Opazo, J. C. (2013). How to Make a Dolphin: Molecular
437 Signature of Positive Selection in Cetacean Genome. *PloS One*, *8*(6), e65491.
438 doi:10.1371/journal.pone.0065491

439 Nguyen, L. T., Schmidt, H. A., Von Haeseler, A., & Minh, B. Q. (2015). IQ-TREE: A fast and
440 effective stochastic algorithm for estimating maximum-likelihood phylogenies.
441 *Molecular Biology and Evolution*. doi:10.1093/molbev/msu300

442 Oh, W. J., & Jacinto, E. (2011). mTOR complex 2 signaling and functions. *Cell Cycle*, *10*(14),
443 2305–2316. doi:10.4161/cc.10.14.16586

444 Parry, D. A. (1949). The structure of whale blubber, and a discussion of its thermal
445 properties. *The Quarterly Journal of Microscopical Science*, *90*(1), 13–25.

446 Pirotta, E., Booth, C. G., Costa, D. P., Fleishman, E., Kraus, S. D., Lusseau, D., … Harwood, J.
447 (2018). Understanding the population consequences of disturbance. *Ecology and*
448 *Evolution*. doi:10.1002/ece3.4458

449 R Core Team. (2014). *R: a language and environment for statistical computing. Vienna,*
450 *Austria*. *R Foundation for Statistical Computing*. Vienna, Austria. Retrieved from
451 http://www.r-project.org/

452 Ranwez, V., Douzery, E. J. P., Cambon, C., Chantret, N., & Delsuc, F. (2018). MACSE v2:
453 Toolkit for the alignment of coding sequences accounting for frameshifts and stop
454 codons. *Molecular Biology and Evolution*. doi:10.1093/molbev/msy159

455 Sarbassov, D. D., Guertin, D. A., Ali, S. M., & Sabatini, D. M. (2005). Phosphorylation and
456 Regulation of Akt/PKB by the Rictor-mTOR Complex. *Science*, *307*(5712), 1098–1101.
457 doi:10.1126/science.1106148

458 Scholander, P. F., Walters, V., Hock, R., & Irving, L. (1950). Body insulation of some arctic and
459 tropical mammals and birds. *The Biological Bulletin*, *99*(2), 225–236.
460 doi:10.2307/1538740

461 Slater, G. S. C., & Birney, E. (2005). Automated generation of heuristics for biological
462 sequence comparison. *BMC Bioinformatics*. doi:10.1186/1471-2105-6-31

463 Thio, L. L., Erbayat-Altay, E., Rensing, N., & Yamada, K. A. (2006). Leptin Contributes to
464 Slower Weight Gain in Juvenile Rodents on a Ketogenic Diet. *Pediatric Research*, *60*(4),
465 413–417. doi:10.1203/01.pdr.0000238244.54610.27

466 Vasseur, D. A., & Yodzis, P. (2004). The color of environmental noise. *Ecology*, *85*(4), 1146–
467 1152. doi:10.1890/02-3122

468 Venn-Watson, S. (2014). Dolphins and Diabetes: Applying One Health for Breakthrough
469 Discoveries. *Frontiers in Endocrinology*, *5*(DEC). doi:10.3389/fendo.2014.00227

470 Venn-Watson, S., Carlin, K., & Ridgway, S. (2011). Dolphins as animal models for type 2
471 diabetes: Sustained, post-prandial hyperglycemia and hyperinsulinemia. *General and*
472 *Comparative Endocrinology*, *170*(1), 193–199. doi:10.1016/j.ygcen.2010.10.005

473 Venn-Watson, S. K., & Ridgway, S. H. (2007). Big brains and blood glucose: common ground

474 for diabetes mellitus in humans and healthy dolphins. *Comparative Medicine*, *57*(4),
475 390–5.

476 Venn-Watson, S., Smith, C. R., Stevenson, S., Parry, C., Daniels, R., Jensen, E., … Wells, R.
477 (2013). Blood-based indicators of insulin resistance and metabolic syndrome in
478 bottlenose dolphins (Tursiops truncatus). *Frontiers in Endocrinology*, *4*(OCT).
479 doi:10.3389/fendo.2013.00136

480 Viscarra, J. a, Vázquez-Medina, J. P., Crocker, D. E., & Ortiz, R. M. (2011). Glut4 is
481 upregulated despite decreased insulin signaling during prolonged fasting in northern
482 elephant seal pups. *American Journal of Physiology. Regulatory, Integrative and*
483 *Comparative Physiology*, *300*, R150–R154. doi:10.1152/ajpregu.00478.2010

484 Wang, Z., Chen, Z., Xu, S., Ren, W., Zhou, K., & Yang, G. (2015). 'Obesity' is healthy for
485 cetaceans? Evidence from pervasive positive selection in genes related to
486 triacylglycerol metabolism. *Scientific Reports*, *5*, 14187. doi:10.1038/srep14187

487 Wang, Z., Xu, S., Du, K., Huang, F., Chen, Z., Zhou, K., … Yang, G. (2016). Evolution of
488 Digestive Enzymes and RNASE1 Provides Insights into Dietary Switch of Cetaceans.
489 *Molecular Biology and Evolution*, *33*(12), 3144–3157. doi:10.1093/molbev/msw191

490 Wells, R. S., McHugh, K. A., Douglas, D. C., Shippee, S., McCabe, E. B., Barros, N. B., &
491 Phillips, G. T. (2013). Evaluation of potential protective factors against metabolic
492 syndrome in bottlenose dolphins: feeding and activity patterns of dolphins in sarasota
493 bay, Florida. *Frontiers in Endocrinology*, *4*, 139. doi:10.3389/fendo.2013.00139

494 Williams, T. M., Friedl, W. a, & Haun, J. E. (1993). The physiology of bottlenose dolphins
495 (Tursiops truncatus): heart rate, metabolic rate and plasma lactate concentration

during exercise. *The Journal of Experimental Biology*, *179*, 31–46.

Williams, T. M., Haun, J., Davis, R. W., Fuiman, L. A., & Kohin, S. (2001). A killer appetite: Metabolic consequences of carnivory in marine mammals. In *Comparative Biochemistry and Physiology - A Molecular and Integrative Physiology* (Vol. 129, pp. 785–796). doi:10.1016/S1095-6433(01)00347-6

Yang, Z. (2007). PAML 4: Phylogenetic analysis by maximum likelihood. *Molecular Biology and Evolution*, *24*(8), 1586–1591. doi:10.1093/molbev/msm088

Ye, J., Gao, Z., Yin, J., & He, Q. (2007). Hypoxia is a potential risk factor for chronic inflammation and adiponectin reduction in adipose tissue of ob/ob and dietary obese mice. *American Journal of Physiology. Endocrinology and Metabolism*, *293*(4), E1118-28. doi:10.1152/ajpendo.00435.2007

Zhang, C., Rabiee, M., Sayyari, E., & Mirarab, S. (2018). ASTRAL-III: Polynomial time species tree reconstruction from partially resolved gene trees. *BMC Bioinformatics*. doi:10.1186/s12859-018-2129-y

Zurano, J. P., Magalhães, F. M., Asato, A. E., Silva, G., Bidau, C. J., Mesquita, D. O., & Costa, G. C. (2019). Cetartiodactyla: Updating a time-calibrated molecular phylogeny. *Molecular Phylogenetics and Evolution*, *133*, 256–262. doi:10.1016/J.YMPEV.2018.12.015

Supplementary Figures

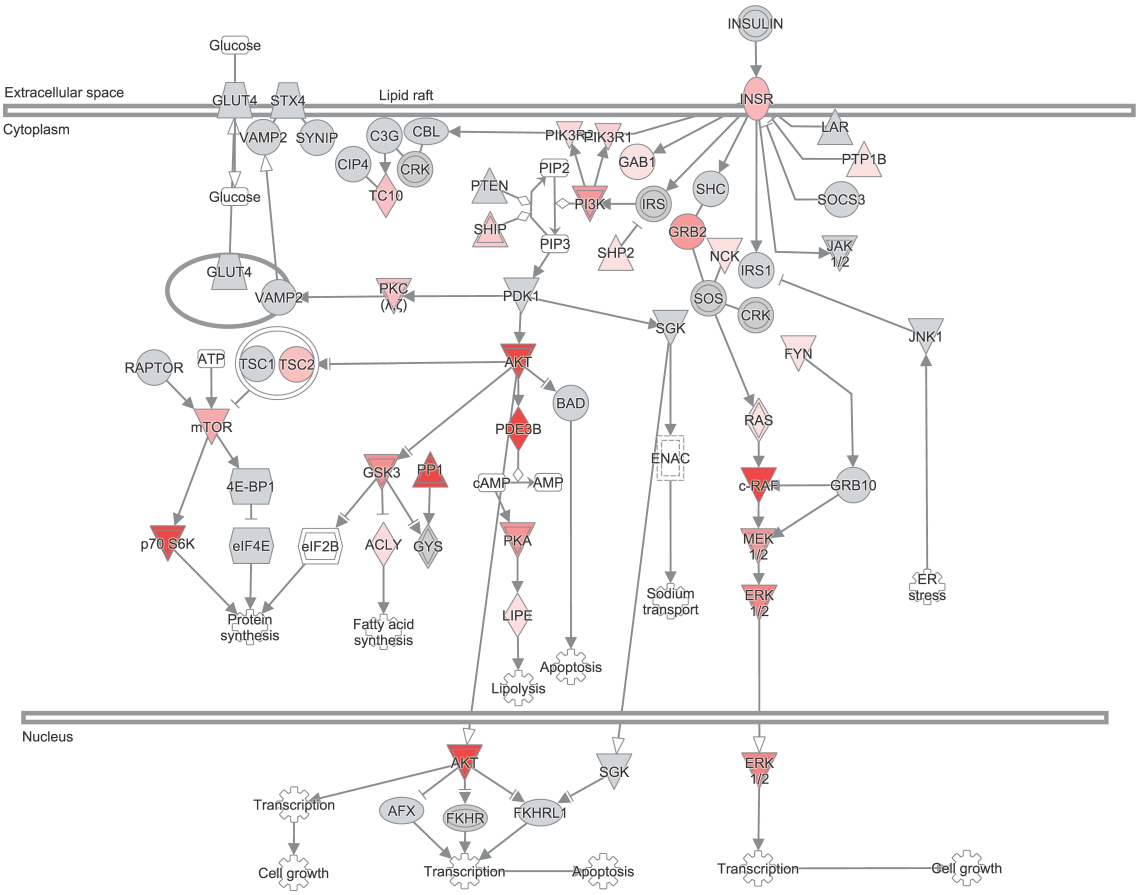

Figure S1. The insulin signaling pathway obtained from Ingenuity Pathway Analysis (IPA) program. Genes in the pathway are colored according to their corresponding 2ΔL value identified by the branch-site model. Intensity of the color is related to the strength of the positive gene selection. Uncolored genes represent those genes with an adjusted p-value > 0.05.

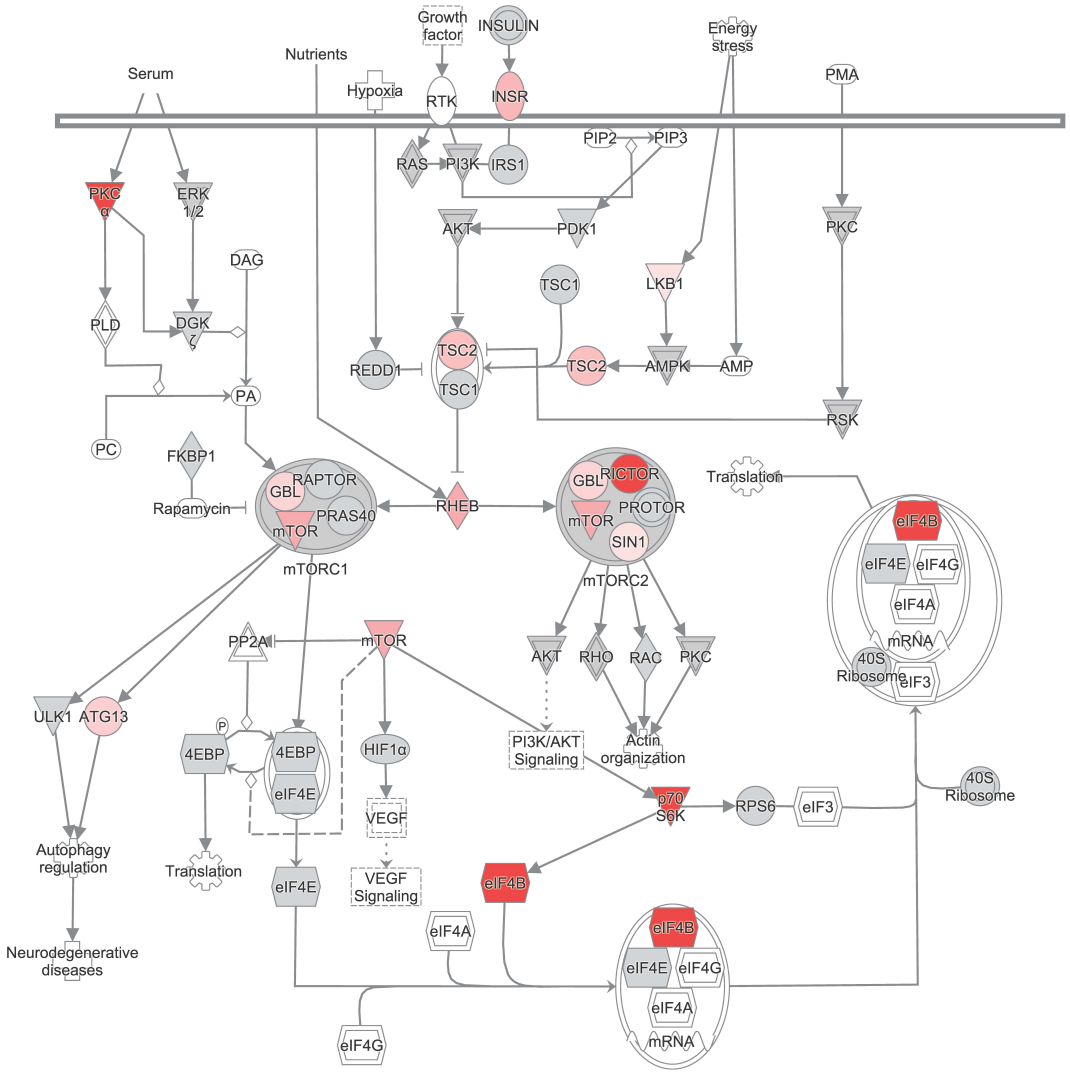

Figure S2. The mTOR signaling pathway obtained for Ingenuity Pathway Analysis (IPA) program. Genes in the pathway are colored according to their corresponding 2ΔL value identified by the branch-site model. Intensity of the color is related to the strength of the positive gene selection. Uncolored genes represent those genes with an adjusted p-value > 0.05.

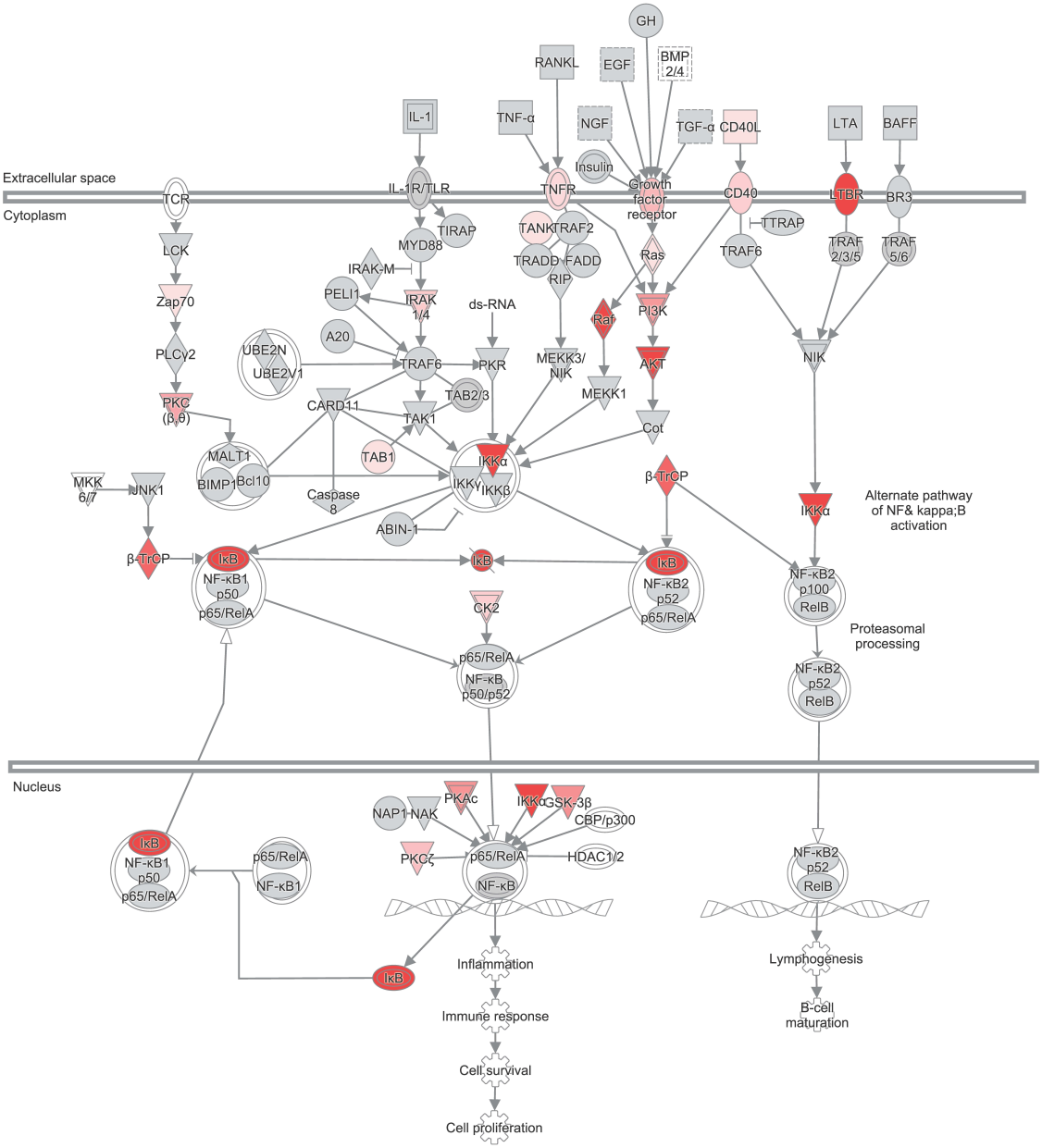

Figure S3. The NF-κB signaling pathway obtained for Ingenuity Pathway Analysis (IPA) program. Genes in the pathway are colored according to their corresponding 2ΔL value identified by the branch-site model. Intensity of the color is related to the strength of the positive gene selection.

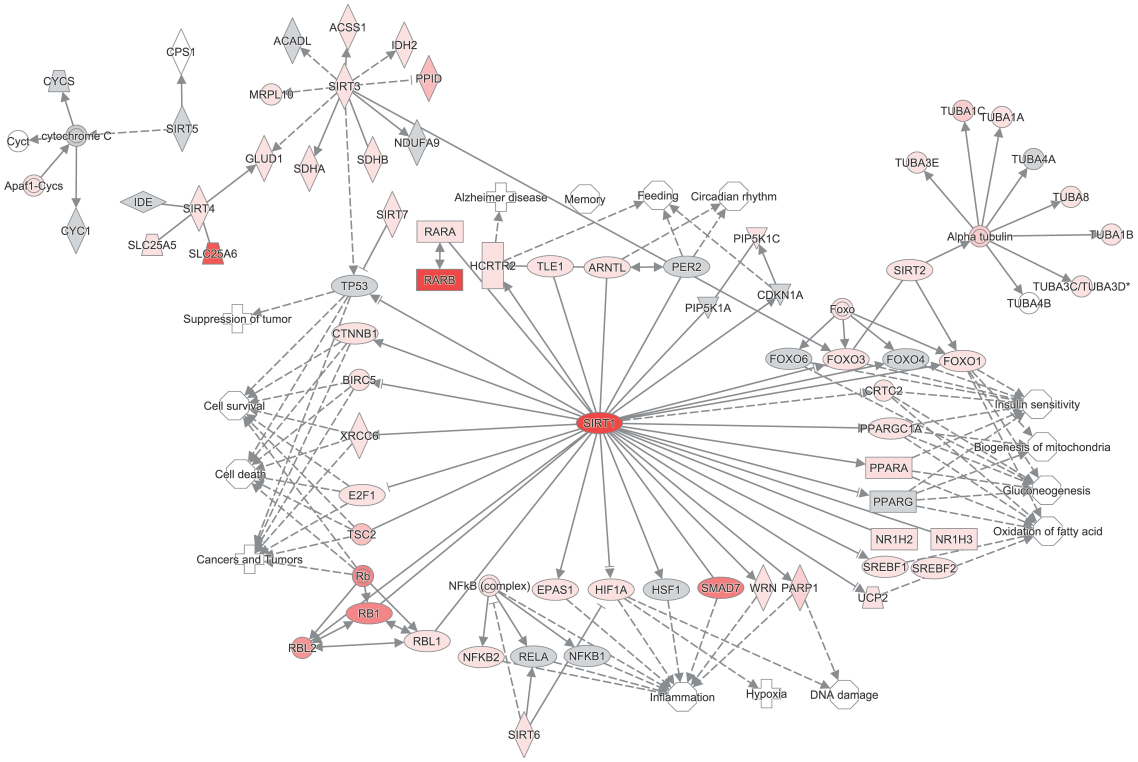

Figure S4. The SIRT signaling pathway created in the Ingenuity Pathway Analysis (IPA) program. Genes in the pathway are colored according to their corresponding 2ΔL value identified by the branch-site model. Intensity of the color is related to the strength of the positive gene selection.

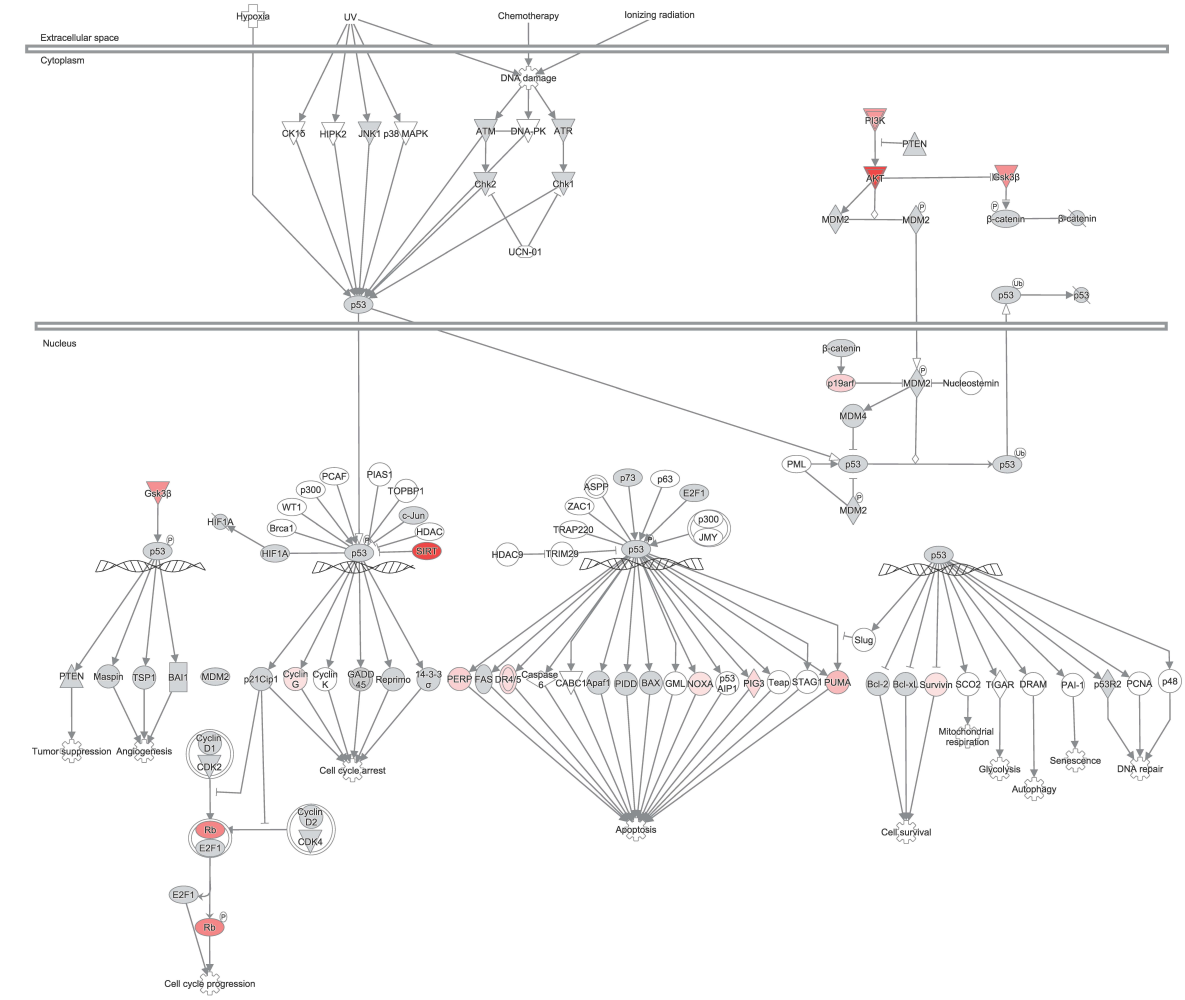

Figure S5. The p53 signaling pathway obtained for Ingenuity Pathway Analysis (IPA) program. Genes in the pathway are colored according to their corresponding 2ΔL value identified by the branch-site model. Intensity of the color is related to the strength of the positive gene selection.

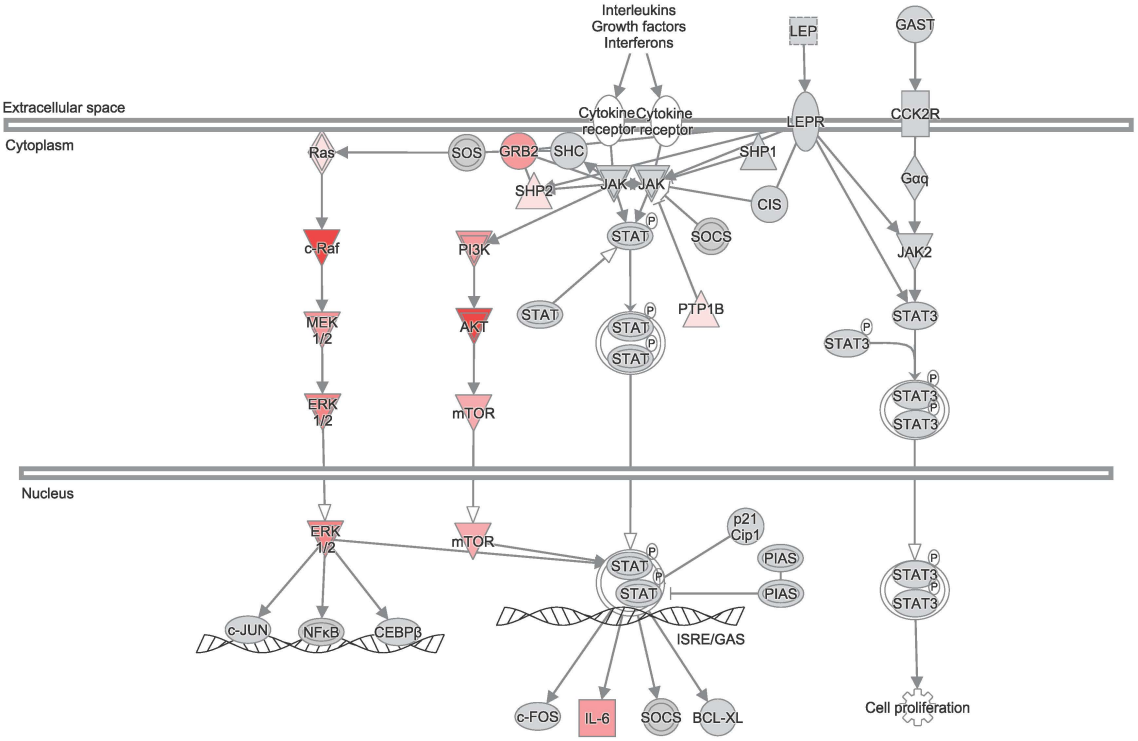

Figure S6. The leptin signaling pathway obtained for Ingenuity Pathway Analysis (IPA) program. Genes in the pathway are colored according to their corresponding 2ΔL value identified by the branch-site model. Intensity of the color is related to the strength of the positive gene selection.

Supplementary Tables

Table S1. The genome assemblies of human, mouse, 16 cetacean species and 37 artiodactyl species downloaded from NCBI.

Group	Species	NCBI accession
Artiodactyla	Ammotragus lervia	GCA_002201775.1
Artiodactyla	Antilocapra americana	GCA_004027515.1
Artiodactyla	Axis porcinus	GCA_003798545.1
Artiodactyla	Beatragus hunteri	GCA_004027495.1
Artiodactyla	Bison bison	GCA_000754665.1
Artiodactyla	Bos indicus	GCA_000247795.2
Artiodactyla	Bos mutus	GCA_000298355.1
Artiodactyla	Bos taurus	GCA_002263795.2
Artiodactyla	Bubalus bubalis	GCA_003121395.1
Artiodactyla	Camelus bactrianus	GCA_000767855.1
Artiodactyla	Camelus dromedarius	GCA_000767585.1
Artiodactyla	Camelus ferus	GCA_000311805.2

Artiodactyla	Capra aegagrus	GCA_000978405.1
Artiodactyla	Capra hircus	GCA_001704415.1
Artiodactyla	Capra sibirica	GCA_003182615.2
Artiodactyla	Capreolus capreolus	GCA_000751575.1
Artiodactyla	Catagonus wagneri	GCA_004024745.1
Artiodactyla	Cervus elaphus	GCA_002197005.1
Artiodactyla	Elaphurus davidianus	GCA_002443075.1
Artiodactyla	Giraffa tippelskirchi	GCA_001651235.1
Artiodactyla	Hemitragus hylocrius	GCA_004026825.1
Artiodactyla	Hippopotamus amphibius	GCA_002995585.1
Artiodactyla	Moschus moschiferus	GCA_004024705.1
Artiodactyla	Odocoileus hemionus	GCA_004115125.1
Artiodactyla	Odocoileus virginianus	GCA_002102435.1
Artiodactyla	Okapia johnstoni	GCA_001660835.1
Artiodactyla	Oryx gazella	GCA_003945745.1
Artiodactyla	Ovis ammon	GCA_003121645.1
Artiodactyla	Ovis aries	GCA_002742125.1
Artiodactyla	Ovis canadensis	GCA_004026945.1
Artiodactyla	Pantholops hodgsonii	GCA_000400835.1
Artiodactyla	Pseudois nayaur	GCA_003182575.1
Artiodactyla	Rangifer tarandus	GCA_004026565.1
Artiodactyla	Saiga tatarica	GCA_004024985.1
Artiodactyla	Sus scrofa	GCA_000003025.6
Artiodactyla	Tragulus javanicus	GCA_004024965.1
Artiodactyla	Vicugna pacos	GCA_000164845.3
Cetacea	Balaenoptera acutorostrata	GCA_000493695.1
Cetacea	Balaenoptera bonaerensis	GCA_000978805.1
Cetacea	Delphinapterus leucas	GCA_002288925.2
Cetacea	Eschrichtius robustus	GCA_002189225.1
Cetacea	Lagenorhynchus obliquidens	GCA_003676395.1
Cetacea	Lipotes vexillifer	GCA_000442215.1
Cetacea	Megaptera novaeangliae	GCA_004329385.1
Cetacea	Mesoplodon bidens	GCA_004027085.1
Cetacea	Monodon monoceros	GCA_004027045.1
Cetacea	Neophocaena asiaeorientalis	GCA_003031525.1
Cetacea	Orcinus orca	GCA_000331955.2
Cetacea	Phocoena phocoena	GCA_003071005.1
Cetacea	Physeter catodon	GCA_002837175.2
Cetacea	Sousa chinensis	GCA_003521335.2
Cetacea	Tursiops aduncus	GCA_003227395.1
Cetacea	Tursiops truncatus	GCA_001922835.1
Outgroup	Homo sapiens	GCA_000001405.27
Outgroup	Mus musculus	GCA_000001635.8

552

553

Table S2. Insulin signaling pathway overlaid with the likelihood-ratio test statistics (2ΔL) between the positive and neutral branch-models as a measure to visualize a pathway effect.

Symbol	**2ΔL**	***p*-value**
4E-BP1	0.000	1.000
ACLY	17.800	<0.001
AFX	0.000	1.000
AKT		
AMP		
Apoptosis		
ATP		
BAD	1.359	0.566
c-RAF	105.387	<0.001
C3G	0.156	1.000
cAMP		
CBL	0.000	1.000
Cell growth		
CIP4	0.003	1.000
CRK		
eIF2B		
eIF4E	0.333	1.000
ENAC		
ER stress		
ERK1/2		
Fatty acid synthesis		
FKHR		
FKHRL1	0.000	1.000
FYN	8.207	0.016
GAB1	11.223	0.004
Glucose		
GLUT4	0.188	1.000
GRB10	3.968	0.139
GRB2	50.205	<0.001
GSK3		
GYS		
INSR	34.960	<0.001
INSULIN		
IRS		
IRS1	0.001	1.000
JAK1/2		
JNK1	0.001	1.000
LAR	0.000	1.000
LIPE	16.254	<0.001
Lipolysis		

MEK1/2		
mTOR	41.010	<0.001
NCK	9.400	0.009
p70 S6K		
PDE3B	105.839	<0.001
PDK1	0.000	1.000
PI3K		
PIK3R1	22.707	<0.001
PIK3R2	20.576	<0.001
PIP2		
PIP3		
PKA		
PKC(λ,ζ)		
PP1		
Protein synthesis		
PTEN	0.019	1.000
PTP1B	14.851	0.001
RAPTOR	0.318	1.000
RAS		
SGK	0.110	1.000
SHC	0.000	1.000
SHIP		
SHP2	9.205	0.009
SOCS3	0.000	1.000
Sodium transport		
SOS		
STX4	0.000	1.000
SYNIP	0.000	1.000
TC10	31.276	<0.001
Transcription		
TSC1	4.121	0.129
Tsc1-Tsc2		
TSC2	31.417	<0.001
VAMP2	3.423	0.185

554

Table S3. mTOR signaling pathway overlaid with the likelihood-ratio test statistics (2ΔL) between the positive and neutral branch-models as a measure to visualize a pathway effect.

Symbol	**2ΔL**	***p*-value**
40S Ribosome-eIF3-mRNA-eIF4A-eIF4B-eIF4E-eIF4G		
40SRibosome		
4EBP	0.000	1.000
4EBP-eIF4E		
Actin organization		

AKT		
AMP		
AMPK		
ATG13	24.238	<0.001
Autophagy regulation		
DAG		
DGKζ	4.209	0.124
eIF3		
eIF4A		
eIF4A-eIF4B-eIF4E-eIF4G		
eIF4B	232.205	<0.001
eIF4E	0.333	1.000
eIF4G		
ERK1/2		
FKBP1	0.010	1.000
GBL	20.882	<0.001
HIF1α	0.000	1.000
Hypoxia		
INSR	34.960	<0.001
INSULIN		
IRS1	0.001	1.000
LKB1	11.489	0.003
mTOR	41.010	<0.001
mTORC1		
mTORC2		
Neurodegenerative diseases		
p70S6K	292.275	<0.001
PA		
PC		
PDK1	0.000	1.000
PI3K		
PIP2		
PIP3		
PKC		
PKCα	383.006	<0.001
PLD		
PMA		
PP2A		
PRAS40	0.000	1.000
PROTOR		
RAC	3.675	0.161
Rapamycin		
RAPTOR	0.318	1.000
RAS		
REDD1	0.000	1.000
RHEB	42.036	<0.001

RHO		
RICTOR	472.142	<0.001
RPS6	1.495	0.531
RSK		
SIN1	10.430	0.005
Translation		
TSC1	4.121	0.129
Tsc1-Tsc2		
TSC2	31.417	<0.001
ULK1	0.000	1.000
VEGF		

555

Table S4. NF-κB signaling pathway overlaid with the likelihood-ratio test statistics (2ΔL) between the positive and neutral branch-models as a measure to visualize a pathway effect.

Symbol	**2ΔL**	***p*-value**
β-TrCP	77.820	<0.001
A20	0.000	1.000
ABIN-1	4.063	0.132
AKT		
B-cell maturation		
BAFF	5.391	0.066
Bcl10	0.000	1.000
Bcl10-Card10-Malt1		
BIMP1	4.177	0.125
BMP2/4		
BR3	5.818	0.053
CARD11	1.116	0.639
Caspase8	0.904	0.723
CBP/p300		
CD40	24.403	<0.001
CD40L	11.317	0.004
Cell proliferation		
Cell survival		
Chuk-Ikbkb-Ikbkg		
CK2		
Cot	0.624	0.876
EGF	3.083	0.219
FADD	0.000	1.000
GH	0.000	1.000
Growth factor receptor		
GSK-3β	55.087	<0.001

HDAC1/2		
IκB		
IkB-NfkB1-RelA		
IkB-NfkB2-RelA		
IKKα	129.661	<0.001
IKKβ	0.014	1.000
IKKγ	2.158	0.368
IL-1		
IL-1R/TLR		
Immune response		
Inflammation		
Insulin		
IRAK1/4		
IRAK-M	0.000	1.000
JNK1	0.001	1.000
LCK	0.000	1.000
LTA	1.123	0.639
LTBR	570.904	<0.001
Lymphogenesis		
MALT1	0.000	1.000
MEKK1	0.000	1.000
MEKK3/NIK		
MKK6/7		
MYD88	1.355	0.566
NAK	0.023	1.000
NAP1	0.208	1.000
NF-κB p50/p52		
NF-κB1	0.000	1.000
NF-κB2 p100	0.000	1.000
NfkB-RelA		
NfkB1-RelA		
NfkB2(p52)-RelB		
NGF	0.145	1.000
NIK		
p65/RelA	0.000	1.000
PELI1	0.000	1.000
PI3K		
PKAc		
PKC(β,θ)		
PKCζ	31.135	<0.001
PKR	0.000	1.000
PLCγ2	0.000	1.000
Raf		
RANKL	1.048	0.670
Ras		
RelB	0.500	0.945

RIP	5.280	0.070
TAB1	9.539	0.008
TAB2/3		
TAK1	1.581	0.504
TANK	8.987	0.010
TCR		
TGF-α	1.477	0.535
TIRAP	0.000	1.000
TNF-α	0.420	1.000
TNFR		
TRADD	2.123	0.375
TRAF2/3/5		
TRAF5/6		
TRAF2	0.000	1.000
TRAF6	1.795	0.444
TTRAP	0.000	1.000
UBE2N	0.011	1.000
Ube2n-Ube2v1		
UBE2V1	0.000	1.000
Zap70	11.445	0.003

556

557

Table S5. SIRT signaling pathway overlaid with the likelihood-ratio test statistics (2ΔL) between the positive and neutral branch-models as a measure to visualize a pathway effect.

Symbol	**2ΔL**	***p*-value**
ACADL	0.000	1.000
ACSS1	0.260	1.000
Alpha tubulin		
Alzheimer disease		
Apaf1-Cycs		
ARNTL	3.815	0.149
Biogenesis of mitochondria		
BIRC5	7.876	0.019
Cancers and Tumors		
CDKN1A	0.000	1.000
Cell death		
Cell survival		
Circadian rhythm		
CPS1		
CRTC2	0.001	1.000

CTNNB1	0.001	1.000
CYC1	0.000	1.000
CYCS	0.000	1.000
Cyct		
cytochrome C		
DNA damage		
E2F1	1.341	0.566
EPAS1	0.001	1.000
Feeding		
Foxo		
FOXO1	0.000	1.000
FOXO3	0.000	1.000
FOXO4	0.000	1.000
FOXO6	0.000	1.000
Gluconeogenesis		
GLUD1	6.982	0.030
HCRTR2	0.000	1.000
HIF1A	0.000	1.000
HSF1	0.000	1.000
Hypoxia		
IDE	0.000	1.000
IDH2	0.000	1.000
Inflammation		
Insulin sensitivity		
Memory		
MRPL10	0.049	1.000
NDUFA9	0.000	1.000
NFkB (complex)		
NFKB1	0.000	1.000
NFKB2	0.000	1.000
NR1H2	0.000	1.000
NR1H3	0.000	1.000
Oxidation of fatty acid		
PARP1	22.597	<0.001
PER2	0.000	1.000
PIP5K1A	0.000	1.000
PIP5K1C	5.059	0.078
PPARA	17.202	<0.001
PPARG	0.000	1.000
PPARGC1A	0.164	1.000
PPID	33.429	<0.001
RARA	0.287	1.000
RARB	242.778	<0.001
Rb		
RB1	61.629	<0.001
RBL1	10.260	0.006

RBL2	53.656	<0.001
RELA	0.000	1.000
SDHA	2.223	0.354
SDHB	14.946	0.001
SIRT1	161.940	<0.001
SIRT2	0.001	1.000
SIRT3	6.500	0.038
SIRT4	0.282	1.000
SIRT5	0.000	1.000
SIRT6	8.713	0.012
SIRT7	0.000	1.000
SLC25A5	2.810	0.254
SLC25A6	87.909	<0.001
SMAD7	64.800	<0.001
SREBF1	4.267	0.120
SREBF2	0.935	0.714
Suppression of tumor		
TLE1	0.000	1.000
TP53	0.000	1.000
TSC2	31.417	<0.001
TUBA1A	4.839	0.088
TUBA1B	0.000	1.000
TUBA1C	25.230	<0.001
TUBA3C/TUBA3D	11.106	0.004
TUBA3E	10.283	0.006
TUBA4A	0.000	1.000
TUBA4B		
TUBA8	0.027	1.000
UCP2	0.000	1.000
WRN	6.106	0.046
XRCC6	0.119	1.000

558

Table S6. P53 signaling pathway overlaid with the likelihood-ratio test statistics (2ΔL) between the positive and neutral branch-models as a measure to visualize a pathway effect.

Symbol	**2ΔL**	***p*-value**
14-3-3σ	0.000	1.000
AKT		
Angiogenesis		
Apaf1	1.169	0.625
Apoptosis		
ASPP		
ATM	2.078	0.382

ATR	0.065	1.000
Autophagy		
BAI1	2.103	0.378
BAX	0.000	1.000
Bcl-2	0.077	1.000
Bcl-xL	0.000	1.000
Brca1		
CABC1		
Caspase 6		
CDK2	0.347	1.000
CDK2-Cyclin D1		
CDK4	0.000	1.000
CDK4-Cyclin D2		
Cell cycle arrest		
Cell cycle progression		
Cell survival		
Chk1	0.000	1.000
Chk2	0.001	1.000
c-Jun	2.366	0.327
CK1δ		
Cyclin D1	0.014	1.000
Cyclin D2	0.010	1.000
CyclinG	13.155	0.001
CyclinK		
DNA damage		
DNA repair		
DNA-PK		
DR4/5		
DRAM		
E2F1	1.341	0.566
E2f1-Rb		
FAS	1.763	0.450
GADD45		
Glycolysis		
GML		
Gsk3β	55.087	<0.001
HDAC		
HDAC9		
HIF1A	0.000	1.000
HIPK2		
Hypoxia		
JMY		
Jmy-p300		
JNK1	0.001	1.000
Maspin	0.223	1.000
MDM2	0.000	1.000

MDM4	0.001	1.000
Mitochondrial respiration		
NOXA	9.495	0.008
Nucleostemin		
p19arf	23.352	<0.001
p21Cip1	0.000	1.000
p300		
p38 MAPK		
p48		
p53	0.000	1.000
p53AIP1		
p53R2	0.018	1.000
p63		
p73	0.564	0.915
PAI-1		
PCAF		
PCNA		
PERP	22.105	<0.001
PI3K		
PIAS1		
PIDD	0.001	1.000
PIG3	18.848	<0.001
PML		
PTEN	0.019	1.000
PUMA	33.998	<0.001
Rb	61.629	<0.001
Reprimo	0.000	1.000
SCO2		
Senescence		
SIRT	161.940	<0.001
Slug		
STAG1		
Survivin	7.876	0.019
Teap		
TIGAR		
TOPBP1		
TRAP220		
TRIM29		
TSP1	0.016	1.000
Tumor suppression		
UCN-01		
WT1		
ZAC1		
β-catenin	0.001	1.000

559

Table S7. Insulin signaling pathway overlaid with the likelihood-ratio test statistics (2ΔL) between the positive and neutral branch-models as a measure to visualize a pathway effect.

Symbol	**2ΔL**	***p*-value**
AKT		
BCL-XL	0.000	1.000
c-FOS	0.000	1.000
c-JUN	2.366	0.327
c-Raf	105.387	<0.001
CCK2R	0.000	1.000
CEBPβ	0.000	1.000
Cell proliferation		
CIS	0.000	1.000
ERK1/2		
Gαq	0.000	1.000
GAST	2.472	0.311
GRB2	50.205	<0.001
IL-6	48.957	<0.001
JAK		
JAK2	0.043	1.000
LEP	0.000	1.000
LEPR	0.000	1.000
MEK1/2		
mTOR	41.010	<0.001
NFκB		
p21Cip1	0.000	1.000
PI3K		
PIAS		
PTP1B	14.851	0.001
Ras		
SHC	0.000	1.000
SHP1	0.000	1.000
SHP2	9.205	0.009
SOCS		
SOS		
STAT		
Stat dimer		
STAT3	2.391	0.323
Stat3 dimer		